

Exploring the Dust Population in Cold Diffuse Clouds

S. J. Gibson^{1,2}, H. Hirashita², A. C. Bell³, M. E. Spraggs^{1,4}, A. Noriega-Crespo⁵, S. Carey⁶, W. T. Reach⁷, C. M. Brunt⁸

¹Western Kentucky U., ²Academica Sinica Inst. of Astron. & Astrophys., ³U. Tokyo, ⁴U. Wisconsin-Madison, ⁵Space Telescope Sci. Inst., ⁶IPAC/Caltech, ⁷SOFIA/USRA, ⁸Exeter U.

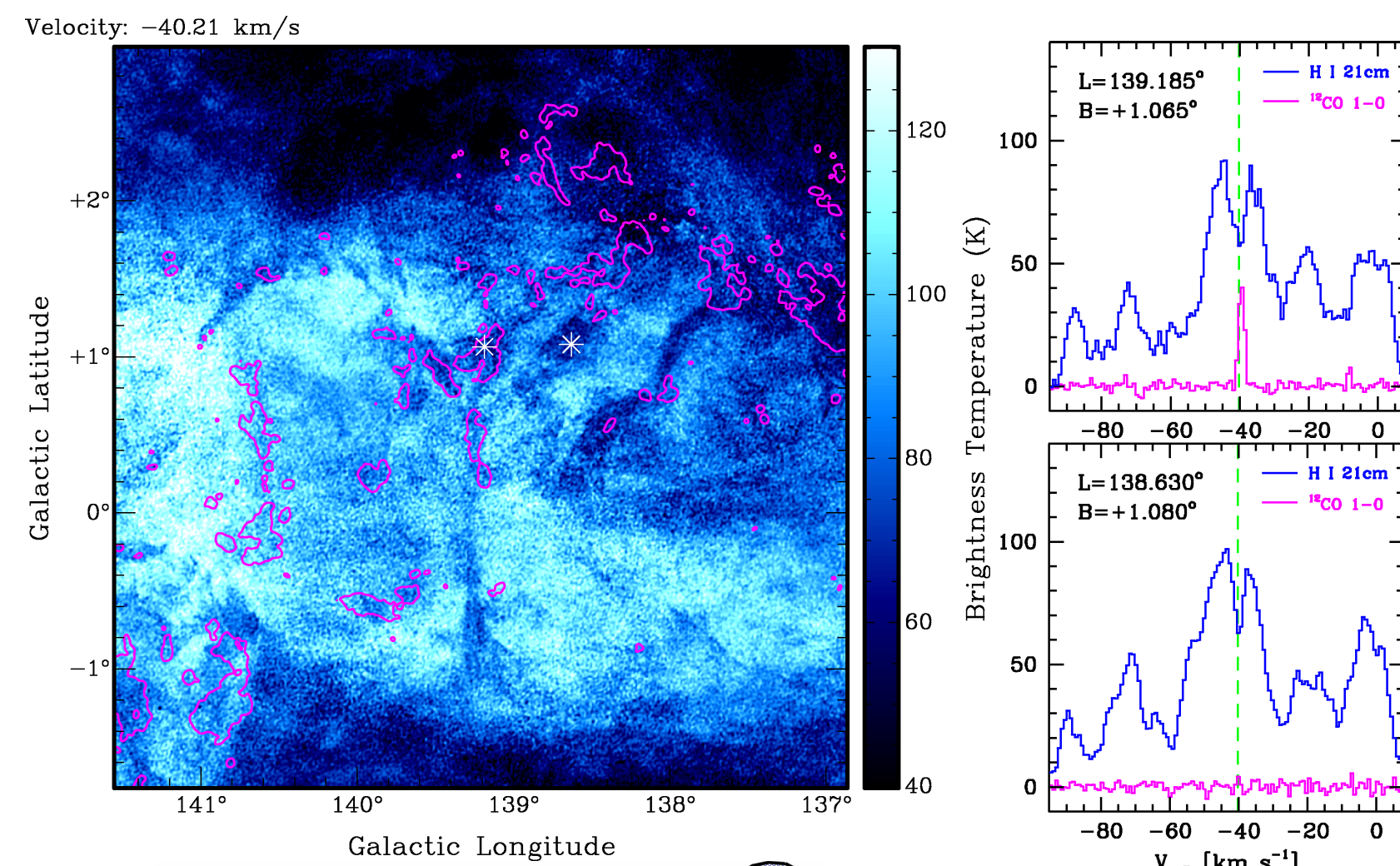


Figure 1. H I self-absorption (HISA) against warmer background H I emission (sketch) arises from atomic gas that is too cold to explain easily if it is outside molecular clouds (Wolfire et al. 2003), and yet HISA shadows often appear separate from CO emission, particularly in the outer Galaxy (Gibson et al. 2000; Gibson 2010). The panels above show CGPS H I (blue; Taylor et al. 2003) and OGS ¹²CO 1-0 (magenta; Heyer et al. 1998). These clouds are ~ 2 kpc away in the Perseus arm, where they may be forming H₂ and CO downstream of the spiral shock before they become dense enough to form new stars (Gibson et al. 2005).

Overview

Cold diffuse clouds (CDCs) are a key transitional phase between the warm, tenuous, ambient interstellar medium of mostly-neutral atomic gas and the colder, denser molecular clouds needed for star formation. However, understanding exactly how CDCs evolve is hampered by observational challenges, as much of their gas is "dark" in H I 21cm and CO 2.6mm spectral line emission surveys, while their dust thermal continuum emission can be faint and hard to distinguish from denser clouds in the same sight line. We have developed methods to identify CDCs via cold H I features in emission and absorption (e.g., Gibson 2010) and to isolate their dust emission from confusing backgrounds (e.g., Spraggs & Gibson 2016) to measure their spectral energy distributions in IR/submm surveys like *AKARI*, *IRAS*, and *Planck*. Using spectral energy distribution (SED) model fits, we aim to constrain the dust temperature, size distribution, composition, and column density and then examine how these may relate to the H I and H₂ content of the CDCs. For example, emission from large grains in thermal equilibrium adds constraints to the gas total column density and shielding of the cloud interior. In addition, very small grain surfaces are important sites for H₂ formation and photoelectric heating. SED studies can thus not only inform us of the evolution of the grains themselves within clouds, but their effect on the clouds' physical state. We have assembled a number of maps of a sample CDC and have begun investigating simple SED model fits for one sight line.

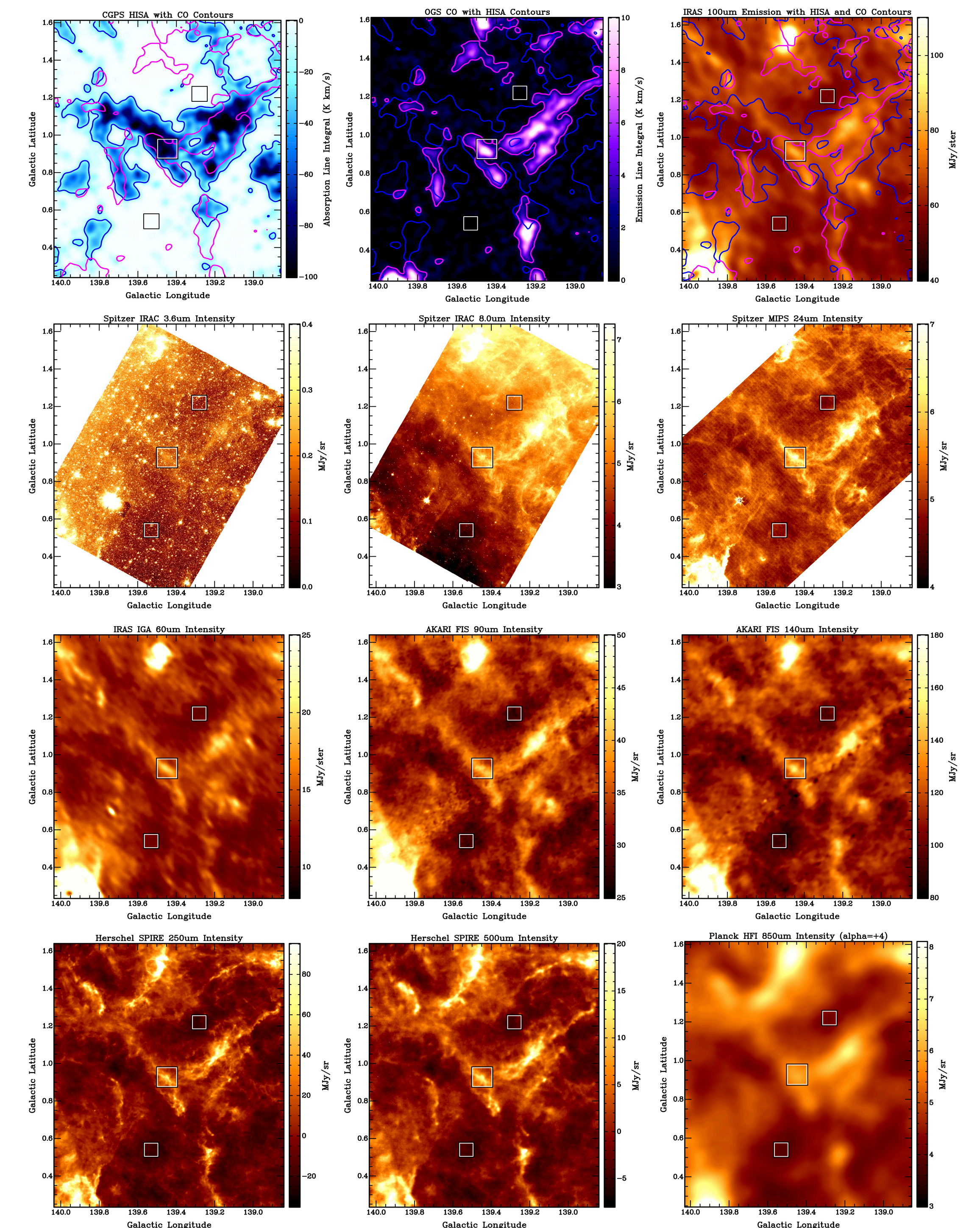


Figure 2. These panels show the region of the current study, which is near the center of **Figure 1**. *Top left*: smoothed line integral of extracted HISA. *Top center*: line integral of associated CO emission. *Top right*: matching *IRAS* 100μm dust emission, with HISA and CO contours. Other panels show a subset of the dust image data assembled for the same region; a full list is given in **Table 1**. The boxes mark one ON and two OFF-cloud areas from which dust emission photometry data were extracted with a 3σ-clipped median statistic; the cloud emission was isolated as the ON minus the averaged OFF brightness, with RMS scatter used as a proxy for measurement uncertainty.

Current Results

- With careful ON-OFF measures to remove backgrounds, photometry from heterogeneous data sets allows fairly detailed constraints on dust SEDs in cold diffuse clouds.
- Long-wavelength ($\lambda > 80 \mu\text{m}$) brightness is consistent with isothermal large-grain emission in a modified blackbody.
- Just below this ($\lambda \sim 60\text{-}70 \mu\text{m}$), very small grains (VSGs) can be fit with a simple MRN power-law distribution.
- At shorter wavelengths ($\lambda < 50 \mu\text{m}$), the MRN model lacks sufficient VSG emission (it also has no PAH component).
- The MRN model H column ($N_{\text{H}} = 1.3 \times 10^{21} \text{ cm}^{-2}$) is broadly consistent with HISA radiative transfer (Gibson et al. 2000) but below that found in combined HISA+CO analyses (e.g., $N_{\text{H}} > 2.4 \times 10^{21} \text{ cm}^{-2}$; Klaassen et al. 2005).

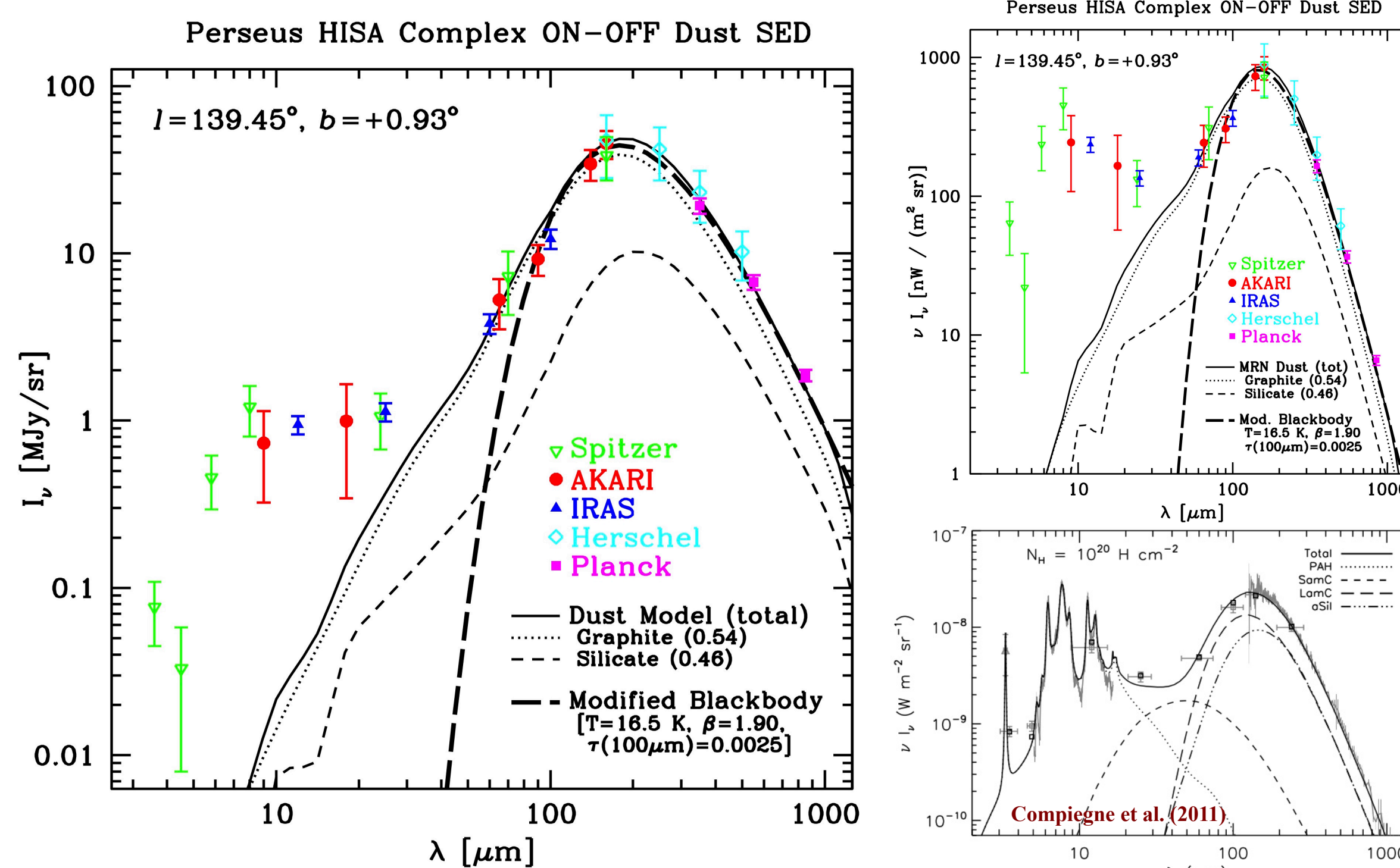


Figure 3. *Left*: Extracted ON-OFF photometry for the sample sight line taken at the positions marked in **Figure 2** from each of the data sets listed in **Table 1**. A simple SED model with Mathis et al. (1977; MRN) grain sizes is shown for a standard interstellar radiation field (Mathis et al. 1983), gas/dust ratio, and metallicity. This model does not have enough VSGs and lacks PAHs, but it fits the longer-wavelength data better than a modified blackbody. *Right*: The same plot, recast in νI_ν units for easier comparison to the more sophisticated DustEM model (Compiegne et al. 2011) to highlight the clear detection of many shorter-wavelength features seen elsewhere.

Future Work

- Incorporate additional short-wavelength data (e.g., *WISE*).
- Try models with more VSG/PAH content (e.g., Weingartner & Draine 2001; Compiegne et al. 2011; Galliano et al. 2011).
- Apply instrument bandpasses and noise RMS maps to fits.
- Broaden model parameters to test for higher extinctions, colder grains in cloud cores, and grain and gas evolution.
- Automate OFF region selection and SED fitting map results vs. position throughout a given cloud, using OFF selection algorithm developed by Spraggs & Gibson (2016).
- Catalog HISA cloud dust and gas properties throughout the Galactic plane (see surveys and maps in Gibson et al. 2015).
- Analyze off-plane clouds showing narrow-line H I emission.

References

- Bell, A. C., et al. 2012, AAS, 219, 349.28
 Cao, Y., et al. 1997, ApJS, 111, 387
 Compiegne, M., et al. 2011, A&A, 525, 1001
 Doi, Y., et al. 2015, PASJ, 67, 50
 Galliano, F., et al. 2011, A&A, 536, A88
 Gibson, S. J. 2010, ASPC, 438, 111
 Gibson, S. J., et al. 2015, IAUS 315, P264
 Gibson, S. J., et al. 2005, ApJ 626, 214
 Gibson, S. J., et al. 2000, ApJ, 540, 851
 Heyer, M. H., et al. 1998, ApJS, 115, 241
 Ishihara, D., et al. 2010, A&A, 514, 1
 Kerton, C. R., & Martin, P. G. 2000, ApJS, 126, 85
 Klaassen, P. D., et al. 2005, ApJ, 631, 1001
 Mathis, J. S., et al. 1983, A&A, 128, 212
 Mathis, J. S., et al. 1977, ApJ, 217, 425
 Miville-Deschenes, M.-A., & Lagache, G. 2005, ApJS, 157, 302
 Molinari, S., et al. 2010, PASP, 122, 314
 Mottram, J. C., & Brunt, C. M. 2010, ASPC, 438, 98
 Planck Collaboration 2016b, A&A, 594, 10
 Planck Collaboration 2016a, A&A, 594, 1
 Spraggs, M. E. & Gibson, S. J. 2016, AAS, 227, 347.16
 Taylor, A. R., et al. 2003, AJ, 125, 3145
 Weingartner, J. C., & Draine, B. T. 2001, ApJ, 548, 296
 Wolfire, M. G., et al. 2003, ApJ, 587, 278

Table 1: Data Sets Used in This Study

Observatory	Instrument	Spectral Band	Beam Size	Surveys/References
DRAO	ST+26m	H I 21 cm line	60"	CGPS ¹
FCRAO	14m	CO 2.6 mm line	45"	OGS ² , EOGs ³
<i>Spitzer</i>	IRAC	3.6, 4.5, 5.8, 8.0 μm	2"	(this work) ⁴
<i>AKARI</i>	IRC	9, 18 μm	6"	IRC ⁵
<i>IRAS</i>	SA	12, 25, 60, 100 μm	70 - 260"	IGA ⁶ , MIGA ⁷ , IRIS ⁸
<i>Spitzer</i>	MIPS	24, 70, 160 μm	7 - 47"	(this work) ⁴
<i>AKARI</i>	FIS	65, 90, 140, 160 μm	63 - 88"	FIS ⁵
<i>Herschel</i>	PACS	70, 160 μm	6 - 13"	Hi-GAL ¹⁰
<i>Herschel</i>	SPIRE	250, 350, 500 μm	18 - 36"	Hi-GAL ¹⁰
<i>Planck</i>	HFI	350, 550, 850 μm	300"	PR2 ¹¹

¹CGPS: Taylor et al. (2003); ²OGS: Heyer et al. (1998); ³EOGS: Mottram & Brunt (2010)

⁴Bell et al. (2012); ⁵IRC: Ishihara et al. (2010); ⁶FIS: Doi et al. (2015); ⁷IGA: Cao et al. (1997)

⁸MIGA: Kerton & Martin (2000); ⁹IRIS: Miville-Deschenes & Lagache (2005)

¹⁰Hi-GAL: Molinari et al. (2010); ¹¹Planck DR2: Planck Consortium (2015a,b)

Support provided by NSF, NASA, WKU, and ASIAA